Journal Pre-proof

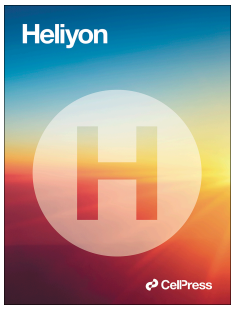

The development of an innovative method to improve the dissolution performance of rivaroxaban

Emma Adriana Ozon, Erand Mati, Oana Karampelas, Valentina Anuta, Iulian Sarbu, Adina Magdalena Musuc, Raul-Augustin Mitran, Daniela C. Culita, Irina Atkinson, Mihai Anastasescu, Dumitru Lupuliasa, Mirela Adriana Mitu

PII: S2405-8440(24)09193-X

DOI: https://doi.org/10.1016/j.heliyon.2024.e33162

Reference: HLY 33162

To appear in: *HELIYON*

Received Date: 5 March 2024

Revised Date: 30 May 2024

Accepted Date: 14 June 2024

Please cite this article as: The development of an innovative method to improve the dissolution performance of rivaroxaban, *HELIYON*, https://doi.org/10.1016/j.heliyon.2024.e33162.

The development of an innovative method to improve the dissolution performance of rivaroxaban

Emma Adriana Ozon[a, #], Erand Mati[b, #], Oana Karampelas[a, #], Valentina Anuta[c,*], Iulian Sarbu[d,*], Adina Magdalena Musuc[e,*], Raul-Augustin Mitran[e], Daniela C. Culita[e], Irina Atkinson[e], Mihai Anastasescu[e], Dumitru Lupuliasa[a], Mirela Adriana Mitu[a]

[a] Department of Pharmaceutical Technology and Biopharmacy, Faculty of Pharmacy, "Carol Davila" University of Medicine and Pharmacy, 6 Traian Vuia Street, 020945 Bucharest, Romania; emma.budura@umfcd.ro (E.A.O.); oana.karampelas@umfcd.ro (O.K.); mirela.mitu@umfcd.ro (M.A.M.); dumitru.lupuliasa@umfcd.ro (D.L.)

[b] "Titu Maiorescu" University, Faculty of Pharmacy, Department of Pharmaceutical Technology, 004051 Bucharest, Romania; erand.mati@prof.utm.ro (E.M.)

[c] Department of Physical and Colloidal Chemistry, Faculty of Pharmacy, "Carol Davila" University of Medicine and Pharmacy, 020956 Bucharest, Romania; valentina.anuta@umfcd.ro (V.A.)

[d] "Titu Maiorescu" University, Faculty of Pharmacy, Department of Pharmaceutical Physics and Biophysics, Drug Industry and Pharmaceutical Biotechnologies, 004051 Bucharest, Romania; iulian.sarbu@prof.utm.ro (I.S.)

[e] "Ilie Murgulescu" Institute of Physical Chemistry, 202 Spl. Independentei, 060021 Bucharest, Romania; amusuc@icf.ro (A.M.M.), raul.mitran@gmail.com (R.A.M.), dculita@icf.ro (D.C.C), iatkinson@icf.ro (I.A.), manastasescu@icf.ro (M.A.)

[#] These authors contributed equally to this work.

Abstract

Recent advancements in the formulation of solid dosage forms involving active ingredient-cyclodextrin complexes have garnered considerable attention in pharmaceutical research. While previous studies predominantly focused on incorporating these complexes into solid states, issues

[*] Corresponding authors e-mail: amusuc@icf.ro (A.M.Musuc); valentina.anuta@umfcd.ro (V. Anuta); iulian.sarbu@prof.utm.ro (I.Sarbu).

regarding incomplete inclusion prompted the exploration of novel methods. In this study, we aimed to develop an innovative approach to integrate liquid-state drug-cyclodextrin inclusion complexes into solid dosage forms. Our investigation centered on rivaroxaban, a hydrophobic compound practically insoluble in water, included in hydroxypropyl-β-cyclodextrin at a 1:1 molar ratio, and maintained in a liquid state. To enhance viscosity, hydroxypropyl-cellulose (2% w/w) was introduced, and the resulting dispersion was sprayed onto the surface of cellulose pellets (CELLETS®780) using a Caleva Mini Coater. The process parameters were meticulously controlled, with atomization air pressure set at 1.1 atmospheres and a fluidizing airflow maintained at 35-45m^3/h. Characterization of the coated cellets, alongside raw materials, was conducted using Fourier Transform Infrared Spectroscopy (FTIR), X-ray diffraction (XRD), scanning electron microscopy (SEM), and differential scanning calorimetry (DSC) analyses. Physicochemical evaluations affirmed the successful incorporation of rivaroxaban into hydroxypropyl-β-cyclodextrin, with the final cellets demonstrating excellent flowability, compressibility, and adequate hardness. Quantitative analysis *via* the HPLC-DAD method confirmed a drug loading of 10 mg rivaroxaban/750 mg coated cellets. *In vitro* dissolution studies were performed in two distinct media: 0.022 M sodium acetate buffer pH 4.5 with 0.2% sodium dodecyl sulfate (mirroring compendial conditions for 10 mg rivaroxaban tablets), and 0.05 M phosphate buffer pH 6.8 without surfactants, compared to reference capsules and conventional tablet formulations. The experimental capsules exhibited similar release profiles to the commercial product, Xarelto® 10 mg, with enhanced dissolution rates observed within the initial 10 minutes. This research presents a significant advancement in the development of solid dosage forms incorporating liquid-state drug-cyclodextrin inclusion complexes, offering a promising avenue for improving drug delivery and bioavailability.

Keywords: inclusion complexes; rivaroxaban; hydroxypropyl-β-cyclodextrin; drug release; dissolution rate; solid dosage forms.

1. Introduction

Recently, the pharmaceutical industry has faced significant challenges in formulating drugs with poor aqueous solubility, such as rivaroxaban (RIV), a potent anticoagulant. Despite their therapeutic potential, these drugs often exhibit limited bioavailability due to their low solubility, which can lead to suboptimal therapeutic outcomes. Cyclodextrins, particularly hydroxypropyl-β-

cyclodextrin (HPβCD), have emerged as promising excipients for enhancing the solubility and bioavailability of poorly soluble drugs by forming inclusion complexes. The preparation and characterization of these inclusion complexes are crucial for optimizing their performance and application. Several studies have investigated the preparation of cyclodextrin-based inclusion complexes to improve the solubility of guest molecules [1-5]. The inclusion of different active pharmaceutical ingredients (API) in the cavity of various cyclodextrins (CDs) has been an important topic for many studies aimed at increasing the solubility, bioavailability, stability, or other disadvantages of the drugs [6-11]. Still, despite numerous data collected in the literature, there are not yet many commercial products based on cyclodextrins inclusion complexes available in the pharmaceutical market. Several reasons stand between the research findings and the pharmaceutical industry production.

Several studies have demonstrated the efficacy of cyclodextrin-based inclusion complexes in improving the solubility and dissolution rates of various drugs. For instance, in a study by Gu and Liu [12], the inclusion of hydroxypropyl-β-cyclodextrin (HPβCD) significantly enhanced the solubility of a hydrophobic compound, thereby improving its bioavailability. Similarly, Lincón-López et al. [13] highlighted the potential of cyclodextrins in pharmaceutical applications, emphasizing their ability to enhance the solubility and stability of drug molecules. Cyclodextrins offer unique molecular structures with hydrophilic exteriors and lipophilic interiors. Many molecules can penetrate the cavity CD to form an inclusion compound. These molecules must meet an important condition, called full or partial conformability to the CD cavity [14-16]. β–CDs are most suitable for pharmaceutical technology because the size of their cavity allows the entrapment of drug molecules. α - CD is generally too small for this purpose, and γ - CD, which is actually a byproduct of the enzymatic degradation of β - CD, is too large [17,18]. The special configuration of CDs gives them the property of being able to trap hydrophobic molecules or the apolar part of amphiphilic molecules in their cavity [19]. Since all APIs have well-established therapeutic dosages that cannot be changed, when incorporating them into the CDs cavity, the complexation phenomenon must take place at minimum molar ratios between API and CD. Taking into account that CDs have a much higher molecular mass than APIs, they become part of the binary system in a larger amount, meaning a greater amount of material must be included in a pharmaceutical form. The inclusion complex turns into the new active ingredient of the product and other excipients must be added to obtain a suitable pharmaceutical system that can be

administered to humans. Unfortunately, at low molar ratios (API:CD) the API incorporation is not complete, but usually only partial complexation is achieved. Most of the data demonstrate that increasing the amount of CD in the complex leads to better inclusion [20-22], but the complex cannot be able to be included in a proper drug, especially an oral solid dosage form. Even if a convenient complexation degree in a low molar ratio is achieved, by using modern technologies such as freeze-drying [23], other disadvantages are encountered. Cyclodextrins are hygroscopic and can easily absorb moisture when exposed to humidity [24]. Therefore, regardless of the method used to prepare the complex, it has a certain water content, which is an important factor in the mechanical properties of materials and in obtaining samples with a specific concentration [25]. Also, all CDs and solid-state inclusion complexes (IC) have very poor flowability, probably due to the enclosed moisture [26-31], which always affects the flow properties of the compression materials and requires either large quantities of fillers and lubricants in the formulation, either the use of advanced excipients which are very expensive or the application of complicated technologies. However, while cyclodextrins offer promising solubility enhancement properties, the integration of inclusion complexes into solid dosage forms remains a challenge. Traditional methods, such as direct compression or wet granulation, may compromise the stability or bioavailability of the drug, limiting its efficacy in achieving optimal dissolution rates. Additionally, the hydrophobic nature of many drugs poses difficulties in achieving uniform dispersion within solid dosage forms. Considering the above drawbacks, the present study aimed to develop a new method that can solve the current problems of pharmaceutical technology and bridge the gap between science and the drug industry regarding the use of CDs in oral solid dosage forms. Our study aims to address this gap by investigating the potential of liquid-state inclusion complexes to enhance API entrapment and formulation characteristics. Specifically, we seek to develop liquid-state inclusion complexes of rivaroxaban (RIV) with hydroxypropyl-β-cyclodextrin (HPβCD) and assess their suitability for oral solid dosage forms.

Rivaroxaban (Figure 1a), a hydrophobic compound with limited aqueous solubility, possesses functional groups such as aromatic rings and carbonyl groups, which contribute to its hydrophobicity and propensity for interactions with other molecules [32]. HPβCD (Figure 1b), on the other hand, is a hydrophilic derivative of cyclodextrin characterized by its hydroxyalkyl substituents, which impart water solubility and facilitate interactions with hydrophobic guest molecules [33].

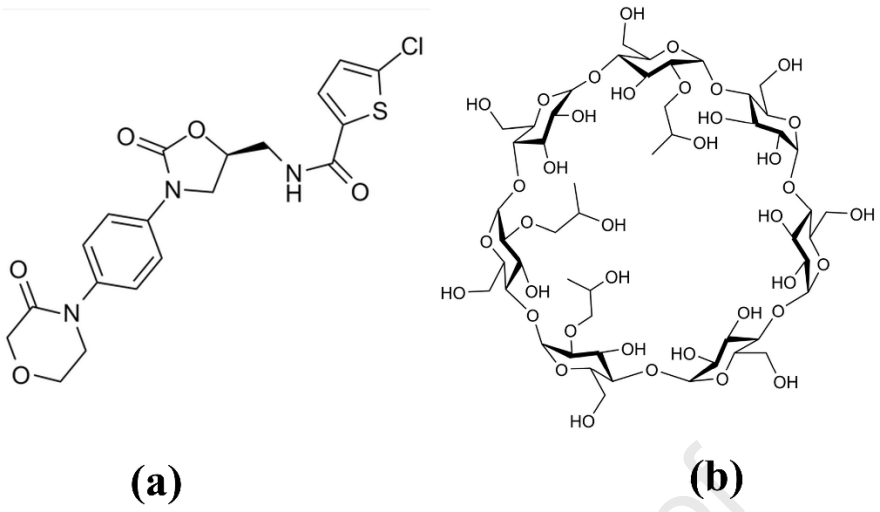

Figure 1. Chemical structures of (a) rivaroxaban and (b) HPβCD.

The structural compatibility between rivaroxaban and HPβCD arises from the complementarity of their molecular structures. The hydrophobic regions of rivaroxaban align with the hydrophobic cavity of HPβCD, allowing for favorable interactions such as van der Waals forces and π-π stacking interactions [34]. Additionally, the hydrophilic exterior of HPβCD promotes aqueous solubility and stabilizes the resulting inclusion complex in solution [35]. Hydrophobic interactions play a crucial role in facilitating the encapsulation of rivaroxaban within the cavity of HPβCD. As rivaroxaban molecules diffuse into the aqueous solution containing HPβCD, they are encapsulated within the hydrophobic cavity through hydrophobic interactions between their hydrophobic moieties and the inner wall of HPβCD. This encapsulation process is driven by the hydrophobic effect, wherein the hydrophobic molecules seek to minimize their exposure to the surrounding aqueous environment by associating with other hydrophobic surfaces [36]. The above-mentioned discussion highlights the structural and molecular basis for the inclusion of rivaroxaban within HPβCD and provides insights into the mechanisms governing inclusion complex formation.

In the proposed method a liquid-state IC, which is intended to have a better entrapment of the API [37,38], is sprayed onto the surface of cellulose pellets, which are then encapsulated in hard gelatin capsules for oral administration. The selected active ingredient was rivaroxaban (RIV) because it has low water solubility, and is included in class II by the Biopharmaceutics Classification System (BCS), meaning its dissolution is the rate-limiting step for absorption [39].

Rivaroxaban, a nonionizable neutral molecule, exhibits consistent solubility across different pH levels. Experimental measurements at 298.15 K have determined its mole fraction solubility in water to be approximately 2.89×10^{-7} [40], while solubility tests in distilled water have yielded a similar value of 3.02×10^{-7} [41]. Khan et al. determined a 5.11 μg/mL solubility in distilled water of RIV. When it was prepared with β-cyclodextrin (βCD) at a molar ratio of 1:2 using the kneading method, the solubility of RIV increased significantly to 42.21 μg/mL, which is 8.26 times higher than that of the pure drug. Additionally, using Soluplus and the solvent evaporation method, the solubility of RIV was dramatically enhanced to 281.27 μg/mL [42]. Also, RIV, a potent anticoagulant substance, was found to have a food-dependent release profile [43]. To increase RIV aqueous solubility and avoid the use of surfactants such as sodium lauryl sulfate in the dosage formulation, it was incorporated in an IC with hydroxypropyl-beta-cyclodextrin (HPβCD), at a minimal molar ratio of 1:1. HPβCD is a synthetic hydroxyalkyl derivative that possesses a very good solubility in water (45% *m/V*), due to the presence of hydrophilic alcohol groups [44]. HPβCD is also well tolerated, being suitable for oral administration [45]. The novelty of our approach lies in leveraging liquid-state inclusion complexes as a means to overcome existing challenges in pharmaceutical technology. By encapsulating rivaroxaban within HPβCD at minimal molar ratios, we aim to enhance its solubility without the need for surfactants. Additionally, to increase the viscosity of the coating dispersion, hydroxypropyl cellulose (HPC) was used at a concentration of 2%. HPC, a cellulose derivative with film-forming properties, acts as a binder and helps to form a protective polymeric film around the cellulose pellets [46]. Although both HPC and HPMC were considered because both are valuable cellulose derivatives in pharmaceutical formulations and offer film-forming properties, binding capabilities, and solubility-promoting characteristics, the choice between them depended on the specific requirements of the formulation, such as solubility requirements, temperature sensitivity, and desired viscosity [47,48], among other factors. One of the main reasons for choosing HPC in the studied formulation is its remarkable solubility in the solvent. HPC dissolves readily in various solvents, allowing efficient formulation preparation. In addition, the solubility-enhancing properties of HPC are of great importance, as they ensure that the API is evenly dispersed throughout the formulation. This improved solubility is crucial to achieve the desired therapeutic effect and consistency of the final product.

2. Materials and methods

2.1. Materials

Micronized RIV (form I) manufactured by Neuland Laboratories Limited was donated by Labormed-Pharma SA, HPβCD was purchased from Global Holding Group Co., Ltd., (Ningbo, China) and HPC from Sigma-Aldrich Chemie GmbH, Germany. Microcrystalline cellulose spheres (Cellets® 780) manufactured by IPC – International Process Center GmbH & Co. KG, Germany, were donated by Harke Romania SCS. All used chemicals and solvents were of analytical reagent grade. A Mettler Toledo AT261 balance (with 0.01 mg sensitivity) was used for weighing the samples.

2.2. Methods

2.2.1. The inclusion complex preparation

The inclusion complex was prepared by the liquid phase method. The equivalent of 1 g of micronized RIV with a D90 of 8µm was dissolved in 30 g of acetone at a temperature of 30° within a sealed glass container, and 3.54 g of HPβCD (respecting the 1:1 molar ratio between the drug and cyclodextrin) was dissolved in 63.46 g of purified water. The aqueous solution was slowly added to the RIV solution with constant mixing, then the mixture was stirred at 750 rpm for 5 hours at room temperature using a Heidolph MR 3001K magnetic stirrer. Acetone, a commonly used organic solvent, was chosen for its ability to dissolve the drug effectively.

2.2.2. The coating dispersion manufacture

After 6 hours, 2 g of HPC was added, and then the mixture was stirred for another hour under the same conditions.

2.2.3. The cellets coating process

The fluid bed system Caleva Mini Coater / Drier 2 produced by Caleva Process Solutions Ltd, UK, was used for the manufacturing process. 75 g of pellets were placed in the fluid bed chamber, and the polymeric film solution was sprayed onto the pellets at a spray rate of 1 ml/min. Air pressures between 0.6 and 2.0 atmospheres were tested in the analysis of the spray patterns. An atomization air pressure of 1.1 atmospheres was deliberately chosen for the spraying process. This specific pressure was selected to ensure a finely dispersed and uniform application of the polymer film to the pellet surface. Spray pattern analysis was performed using a special pad provided by

COLORCON, the design of which was such that it mimicked the conditions of the actual coating process. The height of the spray pattern was carefully kept at 20 cm, which corresponded to the coating process. Upon observation, it was found that the spray had a consistent and uniform circular pattern, forming small droplets that contributed to the creation of a homogeneous film. It should be emphasized that this result is closely related to the specific composition and viscosity of the coating film. The deviation from the optimum atomizing air pressure of 1.1 atmospheres had significant effects. Excessive pressure resulted in fine dispersions with scattered spots, while insufficient pressure led to concentrated areas with larger droplets. This underscores the critical importance of accurately controlling atomizing air pressure to achieve the desired coating properties. At the same time, the process was upheld with a fluidization air flow rate of 35-45 m^3/h and a temperature of 60°C. These operating conditions were carefully maintained to facilitate efficient blending and coating. This dual approach, comprising controlled spraying and continuous fluidization, plays a crucial role in achieving a uniform and precisely desired coating thickness [49] on the cellulose pellets.

2.2.4. The physicochemical characterization of the coated cellets

Fourier transform infrared spectroscopy (FTIR) analysis was carried out using a JASCO FTIR 4100 spectrophotometer (Tokyo, Japan) with solid samples prepared as KBr pellet. The spectra were recorded in the 4000–400 cm^{-1} range.

X-ray diffraction analysis (XRD) was made using a Rigaku Ultima IV diffractometer (Rigaku Co., Tokyo, Japan). The apparatus functioned in parallel beam geometry using a CuKα radiation (λ = 1.5406 Å). The XRD diffractograms were analyzed in 2θ range between 5° and 60° using a speed of 2°/min at step size of 0.02°.

Differential scanning calorimetry (DSC) analyses were performed using a Mettler Toledo DSC 3, under 80 mL min^{-1} nitrogen atmosphere, at a heating rate of 10 °C min^{-1}.

Atomic force microscopy (AFM) measurements were performed in "non-contact" mode with XE-100 device from Park Systems, equipped with decoupled XY / Z scanners. All AFM measurements were performed with NSC36B tips (MicroMasch), with a typical radius of curvature of less than 8 nm, full cone angle of ~40º, height ~15 µm, thickness of ~1 µm, length of ~ 90 µm, width of ~32 µm, force constant of ~ 2 N/m and resonance frequency of ~ 130 kHz. After recording, the images were processed with the XEI program (v 1.8.0, Park Systems). The AFM figures are presented in the so-called "enhanced contrast" mode, in which the color of a pixel is determined

by the color variation of neighboring pixels. For AFM measurements, a drop of each sample (previously suspended in ethanol, in a ratio of 1:10, and collected from supernatant) was placed on specimens of clean and smooth microscope glass substrates (Heinz Herrenz).

FTIR, XRD, DSC and AFM analysis were performed on the coated cellets in comparison to the uncoated cellets, RIV and HPβCD.

The surface and shape characteristics of the cellets were determined by *scanning electron microscopy (SEM)*, using a Hitachi TM4000 plus tabletop scanning electron microscope system (Hitachi High-Tech Corp., Tokyo, Japan). The samples were mounted on SEM aluminum stubs using conductive double-sided adhesive carbon tapes. In order to improve the image quality and resolution of the obtained micrographs, Gold/Palladium in argon sputter coating of the samples was performed, using a SC7620 Mini Sputter Coater (Quorum Technologies Ltd, Ashford, Kent, UK), with a plasma current of 25 mA for 60 seconds. The samples were observed under low-vacuum, using an accelerating voltage of 15 kV, under backscattered electron image (BSE) mode. The coated cellets morphology was examined in comparison to the uncoated cellets powdered with RIV and uncoated cellets powdered with RIV and HPβCD.

2.2.5. The pharmacotechnical evaluation of the coated cellets

The pharmacotechnical properties of the coated cellets were assessed in comparison to the starter cores. All tests were performed three times on each sample.

Particle size distribution was determined by analytical sieving on a CISA Sieve Shaker Mod. RP 10 from Cisa Cedaceria Industrial, Spain. The sample held on each vibrating standard sieve is collected and weighed as 5 g of cellets passes through the sieves after 20 minutes of shaking. The sieves are arranged so that the coarsest are at the top and the finest at the bottom.

Moisture content was verified by thermogravimetric measurement of drying loss, with a HR 73 Mettler Toledo halogen humidity analyzer produced by Mettler-Toledo GmbH, Greifensee, Switzerland.

Flowability was examined by the angle of repose, flowing time and rate as each sample flowed through an orifice with a defined diameter. This study was conducted using an Automated Powder and Granulate Testing System PTG-S3 made by Pharma Test Apparatebau GmbH, Germany.

Volumetric characteristics were investigated with a Vankel Tap Density Tester, fabricated by Vankel Industries Inc., USA. Calculations were made for bulk and tapped density, the Hausner ratio (HR), and the Carr Index (CI). After introducing 10 g of each sample into the graduated

cylinder, the bulk volume was measured. The material was then subjected to a predetermined number of mechanical shocks, to measure the material's tapped volume. The ratio between tapped density and bulk density, or Hausner Ratio (*HR*), and the equation for calculating Carr Index (*CI*), equation (1), are both used to estimate the cellets ability to flow and to be compressed, to uniformly fill the capsules.

$$CI = \frac{100(\rho_f - \rho_0)}{\rho_f} \quad (1)$$

A *HR* value of less than 1.25 shows that the material is freely flowing, and a *CI* value of less than 10 denotes that the material has great flowability and compressibility properties [50,51].

Friability was analyzed with a Vankel friabilator on 2 g of each sample rotated for 5 minutes at a speed of 25 rpm. The de-dusted cellets were weighed again, and the mass loss was calculated and presented as a percentage.

Quantitative determination of rivaroxaban into the coated cellets was performed using an HPLC-DAD method, at 250 nm. Chromatographic separation was accomplished at 45°C on a 100*3.0 mm i.d. Kinetex EVO C18 Core-Shell column (Phenomenex Inc., Torrance, CA, USA) by using a mobile phase composed of 0.1% (v/v) aqueous solution of formic acid and acetonitrile: methanol 1:1 (*v/v*), in a 60:40 (*v/v*) ratio.

2.2.6. Coated cellets encapsulation process

Considering the results of the preformulation studies, 750 mg of cellets must be contained in one capsule in order to achieve a 10 mg RIV concentration per dosage unit. For this purpose, colorless hard gelatin capsules "00" size, manufactured by ACG Associated Capsules Pvt. Ltd and donated by S.C. Slavia Pharm SRL were used as shells of the product. They were filled with content, using a No.00 manual encapsulation device manufactured in-house.

2.2.7. Capsules quality control

Mass uniformity was assessed following the European Pharmacopoeia guidelines [52] by weighing 10 filled capsules and then just the empty shells.

In vitro disintegration time was determined using the disintegration device ELECTROLAB ED-2L, manufactured by ELECTROLAB PVT. LTD, India, in accordance with compendial requirements. Six capsules were placed in each of the six open-ended transparent tubes of the basket rack and tested in purified water at 37 ± 2 °C. A disk was then added on top of each capsule.

The basket rack was then mounted on the apparatus. After the complete disintegration of all six capsules, the apparatus was stopped, and the time was recorded.

In vitro drug release studies were performed in a Vision G2 Classic 6 Dissolution Tester (Teledyne Hanson, Chatsworth, CA, USA), using USP I (basket) apparatus at 37.0 ± 0.5°C and 100 rpm. Using the basket method instead of the paddle method recommended in the Rivaroxaban Tablets USP monograph [53] was preferred to minimize the variability induced by the initial floating tendency of the individual cellets and better simulate the conditions encountered in the gastrointestinal tract when these cellets are ingested as part of a pharmaceutical product. A volume of 900 mL of medium was used for the experiment. Two different dissolution media were tested, *i.e.* 0.022 M sodium acetate buffer pH of 4.5 containing 0.2% sodium dodecyl sulfate (the compendial medium for 10 mg Rivaroxaban tablets), as well as 0.05 M phosphate buffer pH 6.8, without the addition of surface active agents. Aliquots of 1.5 ± 0.1 mL were withdrawn at 5, 10, 15, 20, 30, 45, 60, 90, and 120 min, and immediately replaced with an equal volume of fresh medium at the same temperature. The samples were filtered through a 0.45 μm Teflon® filter, and the drug concentrations were determined by using a validated HPLC method, with UV detection at 250 nm. All evaluations were performed in triplicate. For a better observation of the drug release performance, the developed capsules were compared with the commercial product (Xarelto® 10 mg, Bayer AG, Germany), and two other reference capsules were prepared: capsules containing UC and RIV and capsules with UC, RIV, HPβCD, and HPC in the same amounts as the studied pharmaceutical product.

3. Results and discussion

3.1.The physicochemical characterization of samples

FTIR analysis

The Fourier Transform Infrared (FTIR) spectroscopy analysis conducted in our study not only elucidates the structural composition of the inclusion complex of rivaroxaban (RIV) with hydroxypropyl-beta-cyclodextrin (HPβCD) but also highlights significant novelties in comparison to existing literature. The FTIR spectra of the samples are represented in Figure 2.

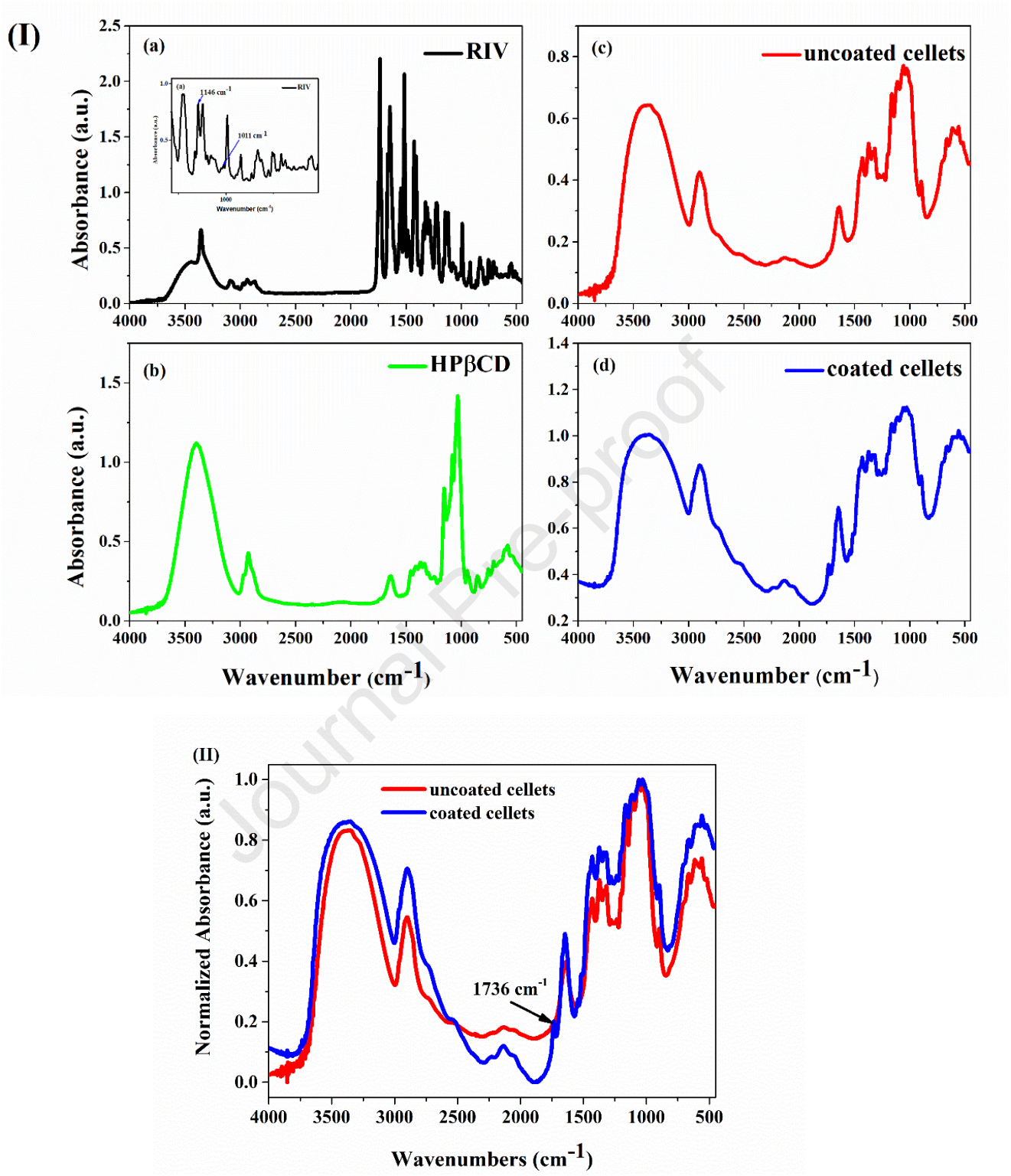

Figure 2. FTIR analyses of the samples (I) (a) RIV (inset the characteristic peaks of RIV, 1200-500 cm^{-1} domain); (b) HPβCD; (c) uncoated cellets; (d) coated cellets; and (II) normalized FTIR analyses for coated and uncoated cellets.

The obtained FTIR spectrum of RIV (Figure FTIR-Ia) showed the characteristic peak at 1011 cm^{-1} confirming the polymorphic form I of RIV. Also, the common peak of forms I was found at 1146 cm^{-1} [54,55]. The peaks located at 3354 cm^{-1} are corresponding to the secondary amide N-H stretching vibration and the medium bands located at 1547 and 1518 cm^{-1} are assigned to N-H bending mode (scissoring). The strong band located at 1738 cm^{-1} is assigned to C=O stretching from the ester group while, the amide group exhibited strong stretching frequencies at 1670 and 1640 cm^{-1}. The strong bands between 1340–1000 cm^{-1} correspond to the C-O-C groups from ethers and esters. The bands between 850–550 cm^{-1} domain were assigned for C-Cl stretching. The obtained FTIR spectrum is in agreement with the RIV form I spectrum reported in the literature [56-59]. Comparatively, while literature references have primarily focused on identifying RIV's crystalline form and validating the structural integrity of HPβCD [56-59], our study uniquely explores the encapsulation process and its implications for pharmaceutical formulation.

In the FTIR spectrum of HPβCD (Figure FTIR-Ib) is observed an intensive broad band which appeared at 3423 cm^{-1} was assigned to O-H group valence vibrations. The peak located at 2927cm^{-1} is assigned to C–H valence vibrations. The bands that appear at 1448 and 1370 cm^{-1} were assigned to asymmetric and symmetric C–H deformation vibrations in the plane from CH_2 and CH_3, respectively. The three bands from 1200–1000 cm^{-1} domain with maxima at 1157, 1084, and 1033 cm^{-1} were assigned to the coupled valence skeletal vibration of C–O, C–O–C, C–C–O, and C–C–C asymmetric groups containing cyclodextrin. The presence of valence and deformation vibrations of glucopyranose units from HPβCD in C1 chair conformation containing α-1,4 linkages of glucose was confirmed by the presence of the two bands at 947 and 855 cm^{-1}, respectively [27,29,60].

Uncoated cellets samples have shown the common FTIR peaks representative of cellulose (Figure FTIR-Ic): the flexural vibrations and the stretching vibrations of intra- and intermolecular hydrogen bonds from the hydroxyl O–H group appear in the range of 3000–3700 cm^{-1} as a broad band with the peak at 3375 cm^{-1}, the C–H stretching vibrations appears at 2894 cm^{-1}, the O–H bending of the absorbed water appears at 1643 cm^{-1}. The peaks at 1424 cm^{-1} and 1373 cm^{-1} are assigned to H–C–H and O–C–H in-plane bending vibrations and C–H deformation vibrations, respectively. The C–O stretching vibrations appear at 1162 cm^{-1}. The O–H bending from the β-

glycosidic linkages between the anhydroglucose units appears at 899 cm^{-1} and the peaks at 666 cm^{-1} were assigned to C–OH out-of-plane bending vibration [61-69].

FTIR spectra of coated cellets (Figure FTIR-Id) did not reveal any obvious RIV peaks (only the peak at 1736 cm^{-1} corresponding to the amide group, Figure FTIR-II), while certain cellets characteristic bands slightly shifted and with different intensities could be recognized. This clearly indicates the successful surrounded of cellets by HPC polymer coating of the drug (included into the HPβCD cavity) loaded pellets. Moreover, our findings underscore the effectiveness of hydroxypropyl cellulose (HPC) polymer coating in encapsulating the RIV-HPβCD inclusion complex, as evidenced by distinct shifts and intensity variations in characteristic cellets bands (Figure FTIR-Id). This innovative approach not only ensures the stability and integrity of the inclusion complex but also holds promise for enhancing the solubility and bioavailability of poorly soluble drugs like RIV.

The FTIR spectroscopy analysis not only corroborates existing literature regarding the structural characteristics of RIV and HPβCD but also introduces novel insights into the encapsulation process and the role of HPC polymer coating in pharmaceutical formulation. These findings represent a significant advancement in drug delivery technology and move forward for further research into optimizing the performance of inclusion complexes in solid dosage forms.

XRD analysis

The X-ray diffraction (XRD) analysis conducted in this study not only confirms the crystalline nature of rivaroxaban (RIV) and the amorphous structure of hydroxypropyl-beta-cyclodextrin (HPβCD) but also highlights novel insights into the efficiency of our formulation approach. The X-ray diffraction spectra of the samples are represented in Figure 3.

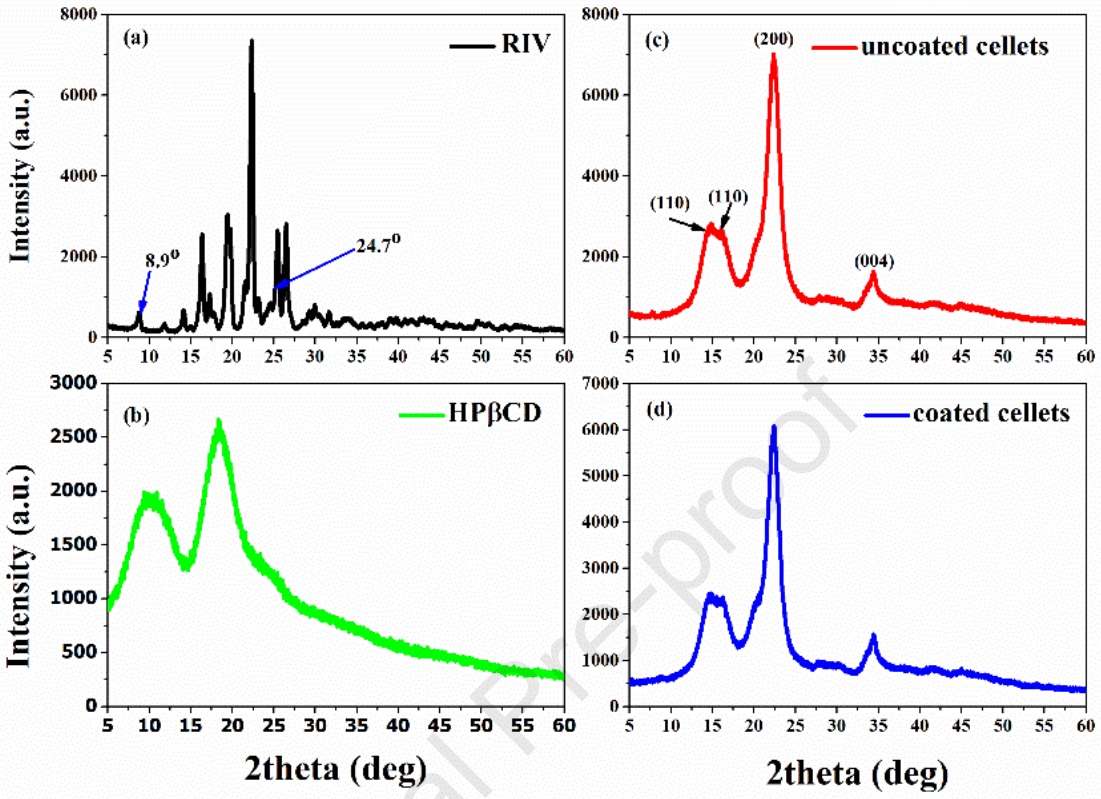

Figure 3. X-ray diffraction pattern of the samples (a) RIV; (b) HPβCD; (c) uncoated cellets and (d) coated cellets.

Analysis of X-ray diffraction patterns (Figure 3a) of RIV showed a distinct crystalline phase with characteristic sharp peaks, confirming the polymorphic form I of RIV [70]. The characteristic peaks of form I were at 8.9° and 24.7°, in agreement with literature [54, 71]. The broad peaks located at 11.6 and between 18–19° which appeared in the X-ray diffractogram of HPβCD (Figure 3b) are not structured, which indicates its amorphous structure [72]. In the XRD pattern of uncoated cellets (Figure 3c), there are diffraction peaks that appear at 2θ = 14.9◦, 16.3◦, 22.5◦, and 34.6◦ that correspond to the following crystallographic planes (110), ($1\bar{1}0$), (200), and (004), respectively following the characteristic X-ray diffraction peaks of cellulose I_β [73-76].

The X-ray diffractogram of coated cellets (Figure 3d) presents no difference compared with the uncoated cellets diffractogram and showed only a reduction in the peak's intensities. This is proof that the cellets were successfully coated with the RIV which was adsorbed onto the carrier surface. Notably, our study uniquely examines the XRD pattern of coated cellets, revealing a

reduction in peak intensities without significant changes in the overall crystalline structure. This observation suggests efficient coating of the cellets with RIV, demonstrating the effectiveness of our formulation strategy. By confirming the crystalline phase of RIV and the amorphous structure of HPβCD, our XRD analysis validates the successful formation of the inclusion complex. The absence of significant changes in the XRD pattern of coated cellets compared to uncoated cellets indicates that the coating process does not alter the crystalline structure of the carrier material. This underscores the efficiency of our formulation approach in preserving the structural integrity of both the drug and carrier components. The XRD analysis presented in this study not only provides novel insights into the structural characteristics of RIV and HPβCD but also underscores the efficiency of our formulation strategy in encapsulating the drug within the carrier matrix. These findings contribute to the advancement of drug delivery systems for poorly soluble drugs and hold promise for enhancing their solubility and bioavailability in pharmaceutical formulations.

DSC analysis

Differential scanning calorimetry (DSC) measurements were performed on the pure drug (RIV), the uncoated cellets, HPβCD and the coated cellets in order to assess the adsorption of RIV molecules on the surface of coated cellets samples (Figure 4).

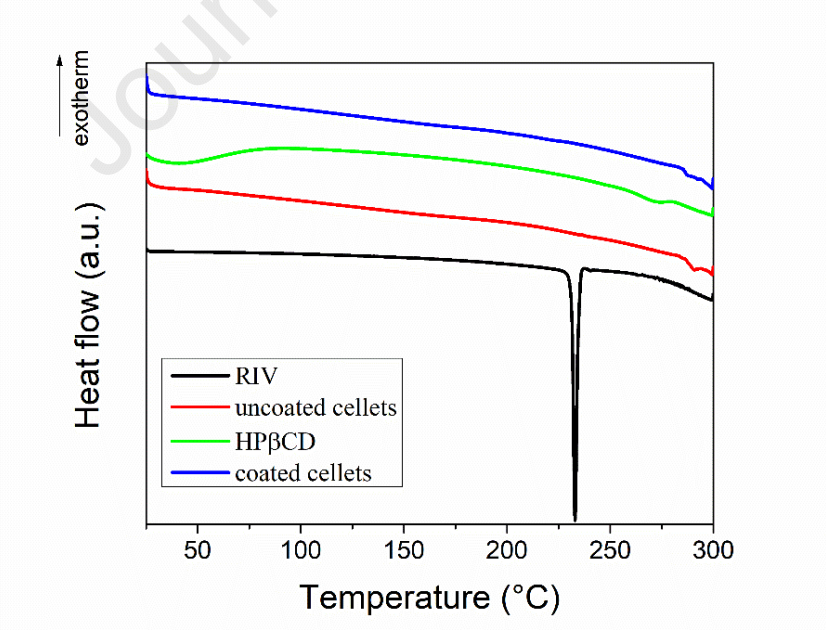

Figure 4. DSC analyses of the samples.

The investigation into the thermal properties of rivaroxaban (RIV)-hydroxypropyl-beta-cyclodextrin (HPβCD) inclusion complexes within solid dosage forms reveals crucial insights into their physical characteristics and interactions, bearing significant implications for pharmaceutical formulation and drug delivery. One of the key observations from thermal analysis studies is the thermal behavior of the inclusion complex as revealed by differential scanning calorimetry (DSC). DSC studies have shown whether the inclusion complex exists in a crystalline or amorphous state, shedding light on the molecular arrangement of rivaroxaban and HPβCD within the complex. Understanding the thermal behavior of the inclusion complex is crucial as it can impact its stability, solubility, and ultimately, its performance in pharmaceutical formulations. The DSC results revealed distinct thermal profiles for each component within the formulation. The sharp endothermic peak observed in the DSC curve of RIV at 232.8 °C is consistent with previous reports and confirms the crystalline nature of the drug [54,59,77]. This finding underscores the importance of understanding the physical characteristics of RIV in pharmaceutical formulations, as crystallinity can significantly impact drug solubility and dissolution kinetics.

Conversely, the broad endothermic event observed in the DSC curve of HPβCD between 25 and 85 °C is attributed to the desorption of physisorbed humidity, highlighting the hygroscopic nature of cyclodextrins [30]. This observation emphasizes the need to consider moisture content in formulation development to ensure product stability and efficacy.

Furthermore, the successful incorporation of the rivaroxaban-HPβCD inclusion complex into pharmaceutical formulations relies on its compatibility with other excipients. Thermal analysis techniques play a crucial role in assessing this compatibility, as they can detect any interactions or incompatibilities between the inclusion complex and formulation components. Notably, the DSC curves of uncoated cellets and coated cellets samples did not exhibit significant transitions, indicating the thermal stability of the HPC cellulose carrier within the analyzed temperature range. In the DSC curve of uncoated cellets, it was observed the appearance of a plateau until 280 °C, because the degradation of cellulose appears at temperatures ranging from 280 to 400 °C, and the carbonation of the residual products over 400 °C [78]. The absence of a distinct melting endotherm in the DSC curve of coated cellets samples suggests that RIV was completely absorbed on the carrier surface. This finding is consistent with our FTIR and XRD analyses, which corroborate the adsorption of RIV molecules onto the carrier surface.

By comparing our DSC results with relevant literature findings, we have provided valuable insights into the physical properties and interactions within the formulation. These insights have important implications for the formulation and performance of solid dosage forms, particularly in terms of drug release kinetics and bioavailability. Thermal analysis techniques have played a pivotal role in assessing this compatibility, as demonstrated by studies by Gill et al. [79] and Ainurofiq et al. [80]. By evaluating the thermal behavior of the inclusion complex in the presence of excipients, researchers can optimize formulation parameters to ensure the stability and efficacy of the final dosage form [81,82].

AFM and SEM analyses

Figure 5 presents the topographic enhanced contrast AFM images, recorded at the scale of (2x2) μm^2, for the samples of interest. Figs. 5(a) and 5(c) are representative of the RIV and HPβCD samples, used further as functional coatings for the cellets, while Figs. 5(b) and 5(d) show the uncoated and coated cellets. Thus, Fig. 5(a) presents the morphology of the RIV, consisting of a sequence of hills (of app. 8-10 nm height) and valleys (of 4-8 nm depth). Nevertheless, in some parts, the RIV sample is disposed more compactly, as in the center of the image, where the height of the clusters is up to ~40 nm in height. Instead, the HPβCD sample, Fig. 5(c), exhibits a more uniform morphology, and an excellent degree of dispersion, leading to a smooth surface with a repetitious structure of nano-pores (visible as small pits). At larger scales, some cavities, of ~8-12 nm depth and a few hundreds of nm in diameter are present on the surface of the HPβCD sample (not shown here). In fact, both the superficial porosity and the presence of superficial cavities are a “fingerprint” of the HPβCD sample, in agreement with other reports [83]. The morphological differences between RIV and HPβCD samples are well expressed by the superposition of the two characteristic line scans (the ones marked by red horizontal lines in Fig. 5(a) and Fig. 5(c)), plotted in Fig. 5(e).

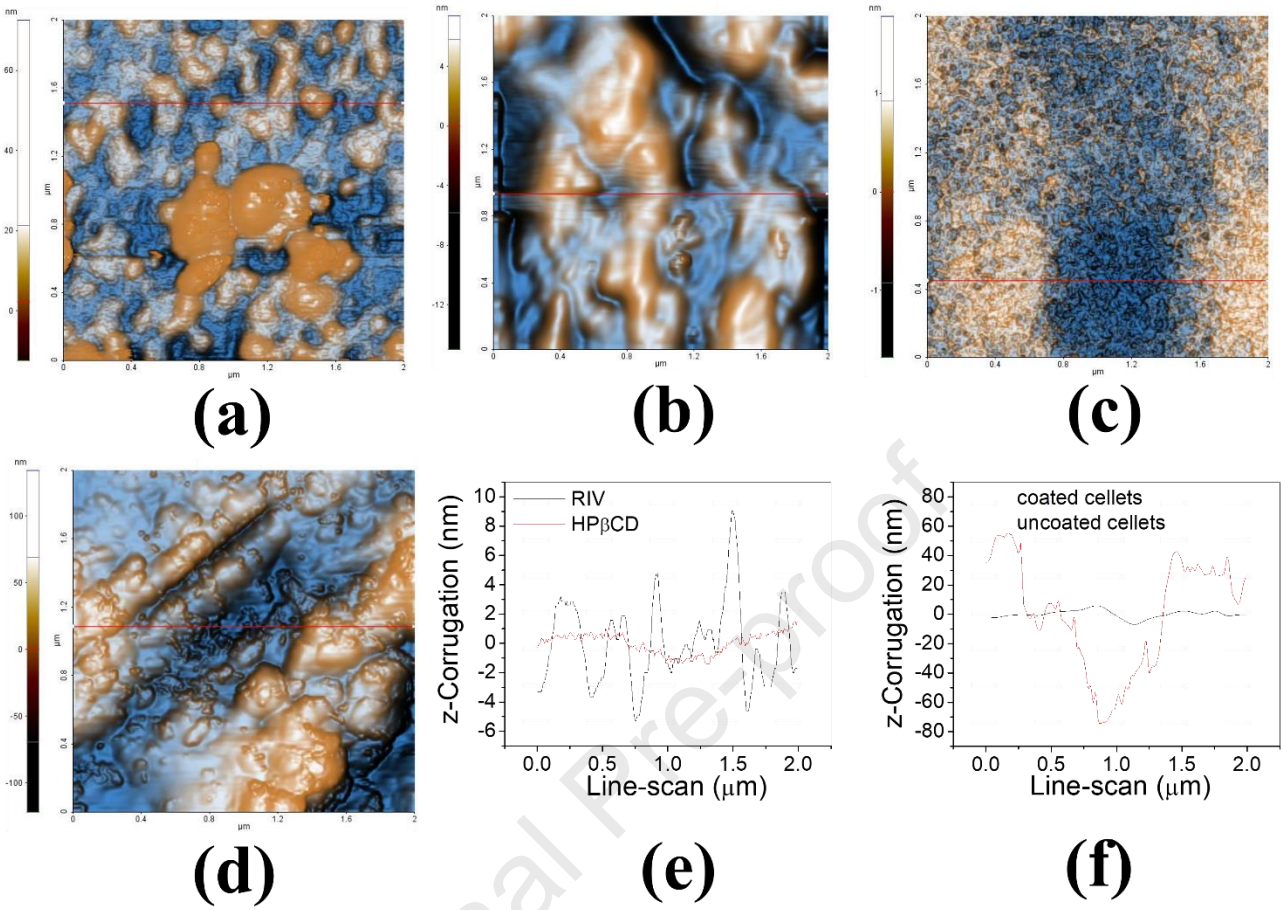

Figure 5. Enhanced-contrast topographic AFM images, recorded at the scale of (2x2)μm^2 for: (a) RIV, (b) uncoated cellets, (c) HPβCD, (d) coated cellets; superimposed characteristic line-scans for the pairs of samples: RIV and HPβCD (e) and, respectively uncoated and coated cellets (f).

From Fig. 5(e) it can be observed that the HPβCD sample is more uniform and smoother with a z-height difference of only a few nm, while in the case of RIV sample, the z-scale difference is one order of magnitude higher. Fig. 5(c) depicts the surface of the uncoated cellets, with the irregularities characteristic of the bare microcrystalline cellulose pellet, having height differences of up to 20 nm. By covering the surface of the cellets, a clear difference in morphology appears in Fig. 5(d), with the coating material forming compact clusters, probably disposed on the ridges/furrows of the underneath microcrystalline cellulose pellet. From the superposition of the two line scans plotted for the bare and coated cellets, collected at the positions indicated by the red horizontal lines from Fig. 5(b) and Fig. 5(d), it can be estimated that the thickness of the coating

layer, covering completely the bare cellets, is ~50-70 nm, as suggested by the z-scale corrugation from Fig. 5(f).

The SEM micrographs are presented in Figure 6.

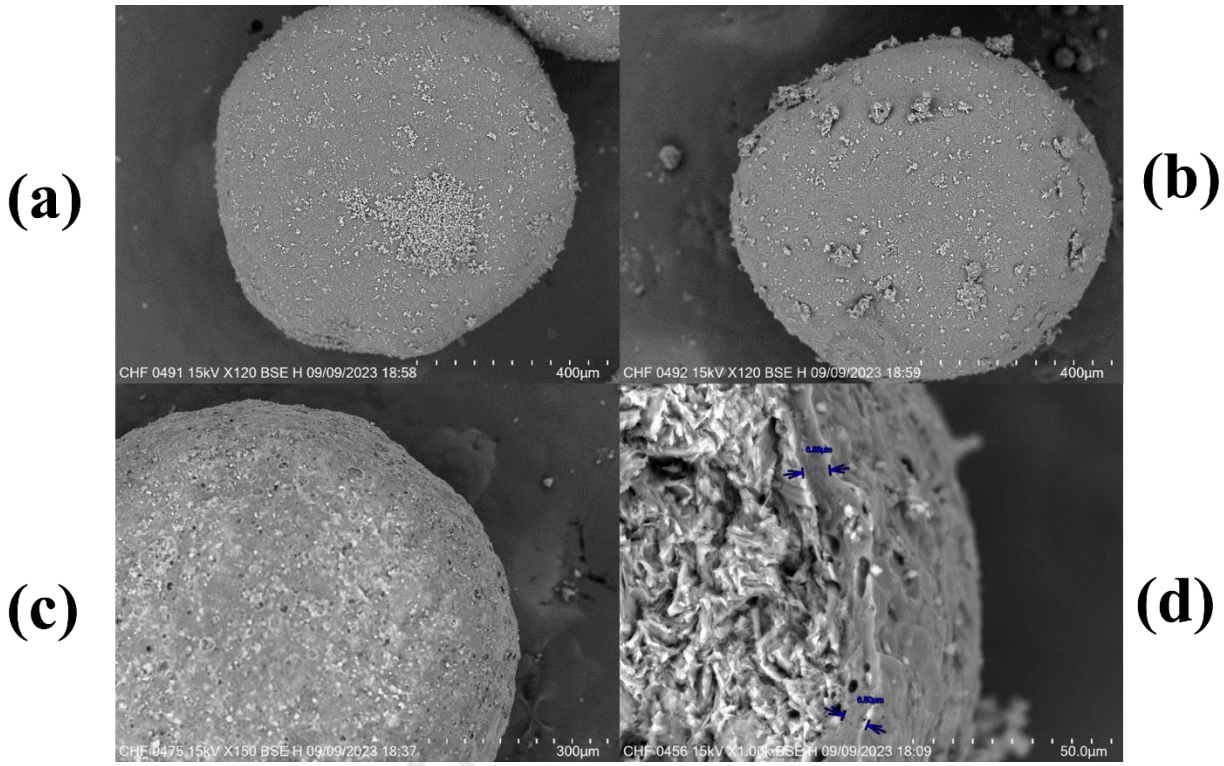

Figure 6. The SEM images of (a) cellets powdered with RIV; (b) cellets powdered with RIV and HPβCD; (c) coated cellets; (d) coated cellets in section

The results from Figure 6 revealed significant differences between film-coated and powdered cellets in terms of the distribution and structure of active components. Film-coated cellets showed a well-defined inclusion complex in which RIV and HPβCD interacted efficiently. This inclusion complex appeared in the form of a uniform film on the surface of the coated cellets, indicating effective adhesion of the active components to their surface. In contrast, the cellets powdered with RIV showed a more irregular distribution of the active ingredient, which appeared to be dispersed on the surface of the cellets in the form of matted particles. In the cellets powdered with RIV and HPβCD, it is observed that the two molecules form agglomerates, indicating the affinity between them, but they are also irregularly distributed.

3.2. The pharmacotechnical evaluation of the coated cellets

For both coated (CC) and uncoated cellets (UC), the highest proportion of spheres is in the range of 600-800 μm, and only 2% of them have sizes above 800 μm. Meanwhile, none of the samples contained particles lower than 600 μm, proving a high uniformity of the dimensions. In addition, the coating layer did not extensively load the cores, forming only a thin film, as the AFM images also demonstrated. The two types of cellets present a narrow distribution of the particle dimensions, with no significant differences between the two samples. Various studies revealed the influence of the pellets' sizes and shapes on the capsule filling behavior, demonstrating that a thicker coat leads to a fluctuating dosage [84-87]. Considering this evidence, it is expected that the RIV CC will have consistent filling ability. In the case of a narrow particle size distribution, a more homogenous dispersion of the blend is attained. A higher moisture content (4.26 ± 0.55%) was found at CC compared to UC (2.84 ± 0.27%). The difference is found in the coating film and is caused by the solvents used in the spreading dispersion. However, the CC complies with Eur. Pharm. standards (≤ 7% moisture) [52], proving that the drying time (5 minutes after the end of spraying) and temperature (60°) were correctly chosen. F. De Leersnyder et al. [88] demonstrated a clear correlation between the parameters of the drying process, the particle size distribution and the moisture of the granules, confirming that the moisture decreases with increasing drying time and temperature, and is also reduced when the particle size distribution is narrow. The flowability of the material is directly related to the amount and distribution of water in the material, and as the moisture content increases, the granules begin to aggregate and fill the capsules unevenly. Maintaining low levels of moisture is crucial since it is concentrated on the CC surface and can affect the mechanical properties of the gelatin capsules, which are vulnerable to humidity due to the hygroscopicity of the gelatin. Both CC and UC exhibited excellent flowability, with an angle of repose of 22.69 ± 1.37° for UC and 23.02 ± 1.58° for CC and flow rates of 1.38 ± 0.22 g/s (UC) and 1.41 ± 0.15 g/s (CC), respectively, when flowing through a 10 mm nozzle without stirring. The similar results registered between the two batches prove that the coating film had no significant effect on the flow behavior. Since the CC showed such a consistent and fast free flow, it can be concluded that the granular material has suitable dynamic properties and will fill the capsules uniformly. Osorio JG et al. [89] or Kurihara and Ichikawa [90] demonstrated that the most important parameter affecting the weight variations in the filled capsules is the flowability of the material. The bulk densities of the samples were different, with a value of 0.870 g/cm^3 for UC

and 0.792 g/cm^3 for CC. The decrease in density after coating was expected, since the SEM images showed the porous and amorphous surface of the CC, given by HPβCD and HPC. After 500 and even 1250 taps, the volumes and the densities of both CC and UC remained unchanged, leading to a HR of 1 and a CI of 0, which reveals ideal volumetric characteristics for capsule filling materials, with excellent flowability and adequate compressibility. This indicates the lack of cohesiveness of the material, with no physical interactions between the cellets. The friability registered for both cellets batches was zero, disclosing a suitable hardness of the coating layer. The results of the friability test prove that the formed film is continuous, without cracks, and has a proper hardness to withstand the subsequent capsule filling process. The determination of the pharmacotechnical properties of the materials is very important as it offers indispensable information on their behavior during the capsule filling process as well as predicting the *in vitro-in vivo* performance of the dosage forms. The quantitative analysis on the coated cellets revealed a content of 10 ± 0.72 mg RIV / 750 mg cellets, proving the consistency of the fabrication method.

3.3. Capsules quality control

Figure 7. Images of studies capsules.

The average mass of the studied capsules was found to be 753 ±12.87 mg. The low variability within the batch shows the uniformity of the process. The excellent flowability and compactness attributes of the cellets lead to an orderly arrangement of the material in the capsule shell. Although the mechanical characteristics of the granules are largely responsible for the mass uniformity, it is nevertheless possible to modify and improve it by using a suitable compression or shaking. The filling capsules disintegrate in the aqueous medium within 293 ± 2.16 seconds, a

desirable performance considering that the objective of the study is to obtain immediate-release dosage forms. To achieve the rapid onset of dissolution and thus the drug absorption, the disintegration process is a critical step.

RIV is a Class II drug in terms of Biopharmaceutics Classification System (BCS), with high permeability and low and pH independent solubility in the pH range 1.2-6.8 (approximately 5–6 μg/mL) [91]. Under fasting conditions, its bioavailability decreases by up to 66% when administered at high doses, whereas dose proportionality and had high oral bioavailability were obtained for all doses under fed conditions [92]. *In-vitro* dissolution testing is a useful tool to assess the variables that affect the rate and extent of drug release from drug products and therefore serve as a substitute for bioavailability studies [93]. The USP dissolution test conditions for RIV recommend the addition of sodium lauryl sulphate (SLS) to the dissolution medium to ensure the sink condition when testing RIV tablets of 10 or 20 mg [53]. However, we proceeded with both the recommended dissolution media, having a pH of 4.5 and 0.2% SLS (that is essentially simulating post-meal conditions), but also with a pH 6.8 buffer in the absence of SLS (simulating the fasted state intestinal conditions), in order to confirm the solubilizing effect of the RIV-HPβCD-HPC complex. The dissolution profiles in the two studied media are represented in Figure 8.

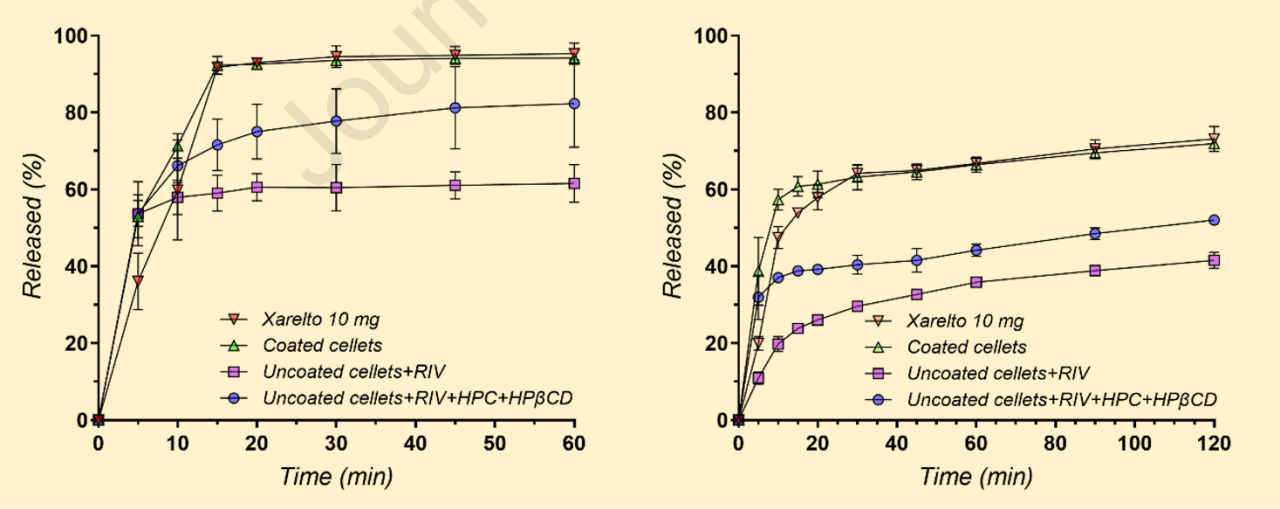

Figure 8. Dissolution profiles in (a) pH 4.5 buffer containing 0.2% SDS (USP compendial medium) and in (b) pH 6.8 buffer.

It is to be noted that the presence of SLS determined a complete release of RIV from the experimental coated cellets within 15 minutes. In the absence of the surfactant, the release was slower, reaching a plateau after about 2 hours and dissolving about 75% of the total RIV amount, thus indicating a solubility-limited release of the drug at about 8.3 mg/mL, slightly higher than the RIV equilibrium solubility in pH 6.8 buffer (reported to be about 6 mg/mL) [94]. In both media, the capsules containing the coated cellets and the commercial product, Xarelto® 10 mg, showed similar release profiles with a higher dissolution rate of the experimental capsules within the first 10 minutes. This can result from a synergistic effect between RIV, HPβCD and HPC. In an aqueous solution, HPC also contributes to a rapid dissolution rate by increasing the wettability of the particles as well as the hydration properties of HPβCD by stabilizing the RIV-HPβCD complex in the aqueous medium [95]. This is also noted that the marketed product contains sodium lauryl sulfate as a surfactant, while the proposed formulation contains only HPβCD and HPC, which are much less aggressive to the human body, providing significant advantages for the safety and tolerability of the product in the context of long-term treatment. A comparison of the curves recorded for the capsules with powdered pellets shows an important difference: the capsules containing HPβCD and HPC show a much higher dissolution rate than the capsules containing RIV only. In this way, the positive influence of HPβCD and HPC on the one hand and the technological process for the coated capsules on the other hand could be precisely determined. By choosing the spray-drying method to coat the cellets with RIV, the contact area between the active ingredient and gastrointestinal fluids is significantly increased, leading to improved release performance. The displayed dissolution behavior suggests that the capsules filled with coated cellets are a potentially safer and more effective option for the administration of RIV.

Conclusions

In conclusion, this study presents a groundbreaking advancement in pharmaceutical technology through the development of a novel method to integrate rivaroxaban-hydroxypropyl-β-cyclodextrin inclusion complexes into solid dosage forms. By maintaining a 1:1 molar ratio in the liquid state, we have successfully improved the dissolution rate of the resulting pharmaceutical capsules. Through comprehensive physical, chemical (including FTIR, XRD, SEM, AFM, and DSC analyses), and pharmacotechnical analyses, we have elucidated the physicochemical

parameters influencing drug dissolution and the *in vitro* performance of the dosage forms, ultimately leading to a refined understanding of the drug release profile. The study underscores the innovative potential of our method in addressing the longstanding challenges associated with poorly soluble drugs, exemplified by rivaroxaban. By employing a novel approach that leverages the encapsulation capabilities of hydroxypropyl-β-cyclodextrin (HPβCD), we have demonstrated a promising strategy for enhancing the solubility and dissolution kinetics of rivaroxaban. Our study contributes novel insights to the existing body of literature by providing a comprehensive characterization of the thermal properties of RIV-HPβCD inclusion complexes in solid dosage forms. By elucidating the thermal behavior of the components and their interactions, our findings lead to advancements in pharmaceutical formulation. This research lays the groundwork for future studies aimed at optimizing drug release profiles and improving the efficacy of poorly soluble drugs, ultimately advancing pharmaceutical science. The present research not only provides a robust solution to the longstanding challenge of formulating poorly soluble drugs but also offers innovative insights into drug-cyclodextrin inclusion complexation. By harnessing the encapsulation capabilities of hydroxypropyl-β-cyclodextrin and optimizing the formulation process, we have demonstrated a transformative approach to enhancing the solubility and dissolution kinetics of rivaroxaban. This method opens up new possibilities for enhancing the bioavailability and therapeutic efficacy of a wide range of poorly soluble drugs, thereby revolutionizing drug formulation and delivery in the pharmaceutical industry.

Moving forward, our study opens up avenues for exploring the broader applicability of cyclodextrin-based formulations in enhancing the solubility and bioavailability of other poorly soluble drugs. Additionally, our innovative approach may inspire further innovations in drug delivery systems, ultimately leading to enhanced therapeutic options in clinical practice. In essence, this research represents a significant step forward in pharmaceutical technology, offering a transformative solution to a longstanding challenge.

Conflicts of Interest

The authors declare no conflict of interest.

CRediT authorship contribution statement

Emma Adriana Ozon: Conceptualization, Methodology, Formal analysis, Investigation, Data curation, Writing – original draft, Writing – review and editing, Visualization.

Erand Mati: Data curation, Formal analysis, Investigation.

Oana Karampelas: Formal analysis, Investigation.

Valentina Anuta: Methodology, Formal analysis, Investigation, Data curation, Writing – original draft.

Iulian Sarbu: Methodology, Formal analysis, Investigation, Data curation, Writing – original draft

Adina Magdalena Musuc: Conceptualization, Methodology, Formal analysis, Investigation, Data curation, Writing – original draft, Writing – review and editing, Visualization, Supervision.

Raul-Augustin Mitran: Formal analysis, Investigation.

Daniela C. Culita: Formal analysis, Investigation.

Irina Atkinson: Formal analysis, Investigation.

Mihai Anastasescu: Formal analysis, Investigation.

Dumitru Lupuliasa: Formal analysis, Investigation, Supervision.

Mirela Adriana Mitu: Formal analysis, Data curation, Visualization, Funding acquisition.

Acknowledgement

This research was partially supported by "Carol Davila" University of Medicine and Pharmacy Bucharest, Romania through Project CNFIS-FDI-2023-F-0708. Publication of this paper was supported by the University of Medicine and Pharmacy Carol Davila, through the institutional program *Publish not Perish*.

Data availability statement

Data will be made available on request.

References

1. Celebioglu, A. Saporito, A.F., Uyar, T. Green Electrospinning of Chitosan/Pectin Nanofibrous Films by the Incorporation of Cyclodextrin/Curcumin Inclusion Complexes:

pH-Responsive Release and Hydrogel Features, *ACS Sustainable Chem. Eng.* 2022, 10, 14, 4758–4769. https://doi.org/10.1021/acssuschemeng.2c00650

2. Yang, G., Li, F., Zhang, H., Yan, H., Gao, S., Fu, Y., Ye, F. Electrospinning for producing antifungal nanofibers consisting of prochloraz/hydroxypropyl-γ-cyclodextrin inclusion complex, *Industrial Crops and Products*, 2024, 211, 118282, https://doi.org/10.1016/j.indcrop.2024.118282.
3. Zhang, Y., Li, F., Guo, G., Xiu, Y., Yan, H., Zhao, L., Gao, S., Ye, F., Fu, Y. Preparation and characterization of betulin/methyl-beta-cyclodextrin inclusion complex electrospun nanofiber: Improving the properties of betulin, *Industrial Crops and Products*, 2024, 209, 117974, https://doi.org/10.1016/j.indcrop.2023.117974.
4. Liu, B., Duan, J., Zhang, Y., Wang, R., Zhao, L., Gao, S., Ye, F., Fu, Y. Preparation and characterization of hexaconazole/hydroxypropyl-gamma-cyclodextrin inclusion complex nanofibers for sustainable agriculture: Improved physicochemical properties and antifungal activity of hexaconazole, *J. Molec. Struct.* 2024, 1299, 137195, https://doi.org/10.1016/j.molstruc.2023.137195.
5. Feng, W, Guo, X., Yang, G., Yao, Y., Zhao, L., Gao, S., Ye, F., Fu, Y. Direct electrospinning for producing multiple activity nanofibers consisting of aggregated luteolin/hydroxypropyl-gamma-cyclodextrin inclusion complex, *Intern. J. Biol. Macromol.* 2024, 270, Part 1, 132344, https://doi.org/10.1016/j.ijbiomac.2024.132344.
6. Szejtli, J. (1998). "Introduction and General Overview of Cyclodextrin Chemistry". *Chem. Rev*. **98** (5): 1743–1754. doi:10.1021/cr970022c
7. Alanzi F., Salah D. Gold nanoparticles incorporated with Cyclodextrins and its application. Journal of Biomaterials and Nanobiotechnology. 2021; 12 (4), 79-97
8. Gu, A., Wheate, N.J. Macrocycles as drug-enhancing excipients in pharmaceutical formulations. *J Incl Phenom Macrocycl Chem* **100**, 55–69 (2021). https://doi.org/10.1007/s10847-021-01055-9
9. Brewster, M. E., Loftsson, T., 'Cyclodextrins as pharmaceutical solubilizers', Advanced Drug Delivery Reviews 59, 2007, p. 645–666
10. Loftsson, T., Masson, M., 'Cyclodextrins in topical drug formulations: theory and practice', Int J Pharm, 225(1-2), 28 August 2001, p. 15–30

11. Musuc A.M., Anuta V, Atkinson I, Sarbu I, Popa VT, Munteanu C, Mircioiu C, Ozon E.A., Nitulescu GM, Mitu MA. Formulation of Chewable Tablets Containing Carbamazepine-β-cyclodextrin Inclusion Complex and F-Melt Disintegration Excipient. The Mathematical Modeling of the Release Kinetics of Carbamazepine. *Pharmaceutics*. 2021; 13(6):915. https://doi.org/10.3390/pharmaceutics13060915.
12. Gu W., Liu Y. Characterization and stability of beta-acids/hydroxypropyl-β-cyclodextrin inclusion complex, *J. Mol. Struct*. **2020**, 1201, 127159, https://doi.org/10.1016/j.molstruc.2019.127159.
13. Rincón-López J, Almanza-Arjona YC, Riascos AP, Rojas-Aguirre Y. Technological evolution of cyclodextrins in the pharmaceutical field. *J Drug Deliv Sci Technol*. **2021** Feb;61:102156. doi: 10.1016/j.jddst.2020.102156.
14. Rincón-López, J.; Almanza-Arjona, Y.C.; Riascos, A.P.; Rojas-Aguirre, Y. Technological Evolution of Cyclodextrins in the Pharmaceutical Field. *J. Drug Deliv. Sci. Technol.* **2021**, *61*, 102156
15. Mura, P. Advantages of the Combined Use of Cyclodextrins and Nanocarriers in Drug Delivery: A Review. *Int. J. Pharm.* **2020**, *579*, 119181
16. Song, L.X.; Bai, L.; Xu, X.M.; He, J.; Pan, S.Z. Inclusion Complexation, Encapsulation Interaction and Inclusion Number in Cyclodextrin Chemistry. *Coord. Chem. Rev.* **2009**, *253*, 1276–1284
17. Gordon B., Leo J. Schep, Mun Y. T., Improvement of the in vitro dissolution of praziquantel by complexation with α-, β- and γ-cyclodextrins, International Journal of Pharmaceutics, Volume 179, Issue 1, 1999, Pages 65-71, https://doi.org/10.1016/S0378-5173(98)00382-2.
18. Gil A., Chamayou, A. Leverd, E. Bougaret, J. Baron, M. et al.. Evolution of the interaction of a new chemical entity, eflucimibe, with gamma-cyclodextrin during kneading process. European Journal of Pharmaceutical Sciences, 2004, 23 (2), p.123-129. ff10.1016/j.ejps.2004.06.002
19. Carrier, R.L.; Miller, L.A.; Ahmed, I. The utility of cyclodextrins for enhancing oral bioavailability. *J. Control Release*, v.123, p.78-99, 2007

20. El-Maradny, H.A; Mortada, S.A.; Kamel, O.A.; Hikal, A.H. Characterization of ternary complexes of meloxicam-HP-beta-CD and PVP or L-arginine prepared by the spray-drying technique. *Acta Pharm*, v.58, p.455-466, 2008
21. Davis, M., Brewster, M. Cyclodextrin-based pharmaceutics: past, present and future. *Nat Rev Drug Discov* 3, 1023–1035 (2004). https://doi.org/10.1038/nrd1576
22. Loftsson, T., Brewster, M.E. Pharmaceutical applications of cyclodextrins: basic science and product development, *Journal of Pharmacy and Pharmacology*, Volume 62, Issue 11, November 2010, Pages 1607–1621, https://doi.org/10.1111/j.2042-7158.2010.01030.x
23. Saharan, V. A.; Kukkar, V.; Kataria, M.; Gera, M.; Choudhury, P. K., Dissolution Enhancement of Drugs Part II: Effect of Carriers, Int J Health Res, September 2009; 2(2): 207-223
24. Crini, G., Fourmentin, S., Fenyvesi, É. *et al.* Cyclodextrins, from molecules to applications. *Environ Chem Lett* **16**, 1361–1375 (2018). https://doi.org/10.1007/s10311-018-0763-2
25. Chattoraj, S.; Daugherity, P.; McDermott, T.; Olsofsky, A.; Roth, J.W.; Tobyn, M. Sticking and picking in pharmaceutical tablet compression: An IQ Consortium review. *J. Pharm. Sci.* **2018**, *107*, 2267–2282
26. Mitu, M.A.; Cretu, E.A.; Novac, M.; Karampelas, O.; Nicoara, A.; Nitulescu, G.; Lupuleasa, D. The Flowing Characteristics of Some Composed Powders Containing Inclusion Complexes in Beta-Cyclodextrin. In *21st Century Pharmacy—Between Intelligent Specialization and Social Responsibility, Proceedings of the 17th Romanian National Congress of Pharmacy, 26–29 September 2018, Bucharest, Romania,* 17th ed.; Draganescu, D., Arsene, A., Eds.; Filodiritto Proceedings, Bologna, Italy, 2018; pp. 129–133
27. Balaci T, Velescu B, Karampelas O, Musuc AM, Nițulescu GM, Ozon EA, Nițulescu G, Gîrd CE, Fița C, Lupuliasa D. Physico-Chemical and Pharmaco-Technical Characterization of Inclusion Complexes Formed by Rutoside with β-Cyclodextrin and Hydroxypropyl-β-Cyclodextrin Used to Develop Solid Dosage Forms. *Processes*. 2021; 9(1):26. https://doi.org/10.3390/pr9010026
28. Ozon EA, Novac M, Gheorghe D, Musuc AM, Mitu MA, Sarbu I, Anuta V, Rusu A, Petrescu S, Atkinson I, et al. Formation and Physico-Chemical Evaluation of Nifedipine-

hydroxypropyl-β-cyclodextrin and Nifedipine-methyl-β-cyclodextrin: The Development of Orodispersible Tablets. *Pharmaceuticals*. 2022; 15(8):993. https://doi.org/10.3390/ph15080993

29. Novac M, Musuc AM, Ozon EA, Sarbu I, Mitu MA, Rusu A, Petrescu S, Atkinson I, Gheorghe D, Lupuliasa D. Design and Evaluation of Orally Dispersible Tablets Containing Amlodipine Inclusion Complexes in Hydroxypropyl-β-cyclodextrin and Methyl-β-cyclodextrin. *Materials*. 2022; 15(15):5217. https://doi.org/10.3390/ma15155217
30. Novac M, Musuc AM, Ozon EA, Sarbu I, Mitu MA, Rusu A, Gheorghe D, Petrescu S, Atkinson I, Lupuliasa D. Manufacturing and Assessing the New Orally Disintegrating Tablets, Containing Nimodipine-hydroxypropyl-β-cyclodextrin and Nimodipine-methyl-β-cyclodextrin Inclusion Complexes. *Molecules*. 2022; 27(6):2012. https://doi.org/10.3390/molecules27062012
31. Tiwari G, Tiwari R, Rai AK. Cyclodextrins in delivery systems: Applications. J Pharm Bioallied Sci. 2010 Apr;2(2):72-9. doi: 10.4103/0975-7406.67003.
32. Meng Y, Tan F, Yao J, Cui Y, Feng Y, Li Z, Wang Y, Yang Y, Gong W, Yang M, Kong X, Gao C. Preparation, characterization, and pharmacokinetics of rivaroxaban cocrystals with enhanced in vitro and in vivo properties in beagle dogs. Int J Pharm X. 2022 May 21;4:100119. doi: 10.1016/j.ijpx.2022.100119.
33. Shalaby KS, Ismail MI, Lamprecht A. Cyclodextrin Complex Formation with Water-Soluble Drugs: Conclusions from Isothermal Titration Calorimetry and Molecular Modeling. AAPS PharmSciTech. 2021 Aug 31;22(7):232. doi: 10.1208/s12249-021-02040-8.
34. Wani TA, AlRabiah H, Bakheit AH, Kalam MA, Zargar S. Study of binding interaction of rivaroxaban with bovine serum albumin using multi-spectroscopic and molecular docking approach. Chem Cent J. 2017 Dec 20;11(1):134. doi: 10.1186/s13065-017-0366-1.
35. Aiassa V, Garnero C, Zoppi A, Longhi MR. Cyclodextrins and Their Derivatives as Drug Stability Modifiers. Pharmaceuticals (Basel). 2023 Jul 28;16(8):1074. doi: 10.3390/ph16081074.
36. Hillyer M.B., Gibb B.C. Molecular Shape and the Hydrophobic Effect, *Annual Review of Physical Chemistry* **2016**, 67(1):307-329, DOI: 10.1146/annurev-physchem-040215-112316,

37. Challa, R., Ahuja, A., Ali, J. *et al.* Cyclodextrins in drug delivery: An updated review. *AAPS PharmSciTech* **6**, 43 (2005). https://doi.org/10.1208/pt060243
38. Memisoglu E, Bochot A, Sen M, Charon D, Duchene D, Hincal AA. Amphiphilic beta-cyclodextrins modified on the primary face: synthesis, characterization, and evaluation of their potential as novel excipients in the preparation of nanocapsules.*J Pharm Sci.* 2002;91:1214–1224
39. Kushwah V, Arora S, Tamás Katona M, Modhave D, Fröhlich E, Paudel A. On Absorption Modeling and Food Effect Prediction of Rivaroxaban, a BCS II Drug Orally Administered as an Immediate-Release Tablet. Pharmaceutics. 2021 Feb 20;13(2):283. doi: 10.3390/pharmaceutics13020283
40. Metre, S., Mukesh, S., Samal, S.K., Chand, M., Sangamwar, A.T. Enhanced biopharmaceutical performance of rivaroxaban through polymeric amorphous solid dispersion, Mol. Pharm. 15 (2) (2018) 652–668, https://doi.org/10.1021/acs.molpharmaceut.7b01027.
41. Jeong, J.-S., Ha, E.-S., Park, H., Lee, S.-K., Kim, J.-S., Kim, M.-S. Measurement and correlation of solubility of rivaroxaban in dichloromethane and primary alcohol binary solvent mixtures at different temperatures, J. Mol. Liq., 2022, 357, 119064, https://doi.org/10.1016/j.molliq.2022.119064.
42. Khan, W. H., Asghar, S., Khan, I. U., Irfan, M., Alshammari, A., Rajoka, M. S. R., Munir, R., Shah, P. A., Khalid, I., Razzaq, F. A., Khalid, S. H. Effect of hydrophilic polymers on the solubility and dissolution enhancement of rivaroxaban/beta-cyclodextrin inclusion complexes, Heliyon, 2023, 9(9), e19658, https://doi.org/10.1016/j.heliyon.2023.e19658.
43. Takács-Novák K., Szőke V., Völgyi G., Horváth P., Ambrus R., Szabó-Révész P. Biorelevant solubility of poorly soluble drugs: Rivaroxaban, furosemide, papaverine and niflumic acid. *J. Pharm. Biomed. Anal.* 2013;83:279–285. doi: 10.1016/j.jpba.2013.05.011
44. Jambhekar SS, Breen P. Cyclodextrins in pharmaceutical formulations I: structure and physicochemical properties, formation of complexes, and types of complex. Drug Discov Today. 2016;21:356–62
45. D'Aria, F., Pagano, B. & Giancola, C. Thermodynamic properties of hydroxypropyl-β-cyclodextrin/guest interaction: a survey of recent studies. *J Therm Anal Calorim* **147**, 4889–4897 (2022). https://doi.org/10.1007/s10973-021-10958-1

46. Qiao Chen, Jingyun Weng, Gabriele Sadowski, Yuanhui Ji. Influence Mechanism of Polymeric Excipients on Drug Crystallization: Experimental Investigation and Chemical Potential Gradient Model Analysis and Prediction. *Crystal Growth & Design* **2023**, *23* (5) , 3862-3872. https://doi.org/10.1021/acs.cgd.3c00314
47. Sanders, J. C.; Breadmore, M. C.; Kwok, Y. C.; Horsman, K. M.; Landers, J. P. (2003). "Hydroxypropyl Cellulose as an Adsorptive Coating Sieving Matrix for DNA Separations: Artificial Neural Network Optimization for Microchip Analysis". *Analytical Chemistry*. **75** (4): 986–994
48. Marani, P.L., Bloisi, G.D. & Petri, D.F.S. Hydroxypropylmethyl cellulose films crosslinked with citric acid for control release of nicotine. *Cellulose* **22**, 3907–3918 (2015). https://doi.org/10.1007/s10570-015-0757-1
49. Murthy Dwibhashyam VS, Ratna JV. Key formulation variables in tableting of coated pellets. Indian J Pharm Sci. 2008 Sep;70(5):555-64. doi: 10.4103/0250-474X.45391. PMID: 21394249; PMCID: PMC3038277.
50. Moreton, C. Functionality and performance of excipients in a quality-bydesign world, part VIII: Excipient specifications. *Am. Pharm. Rev.* **2010**, *13*, 46–50
51. Fița AC, Secăreanu AA, Musuc AM, Ozon EA, Sarbu I, Atkinson I, Rusu A, Mati E, Anuta V, Pop AL. The Influence of the Polymer Type on the Quality of Newly Developed Oral Immediate-Release Tablets Containing Amiodarone Solid Dispersions Obtained by Hot-Melt Extrusion. *Molecules*. 2022; 27(19):6600. https://doi.org/10.3390/molecules27196600
52. Council of Europe. *European Pharmacopoeia*, 10th ed.; EDQM, Council of Europe: Strasbourg, France, 2019
53. Rivaroxaban Tablets. In USP-NF, Rockville, MD: May 1, 2023, doi: https://doi.org/10.31003/USPNF_M7232_02_01
54. Parth S. Shaligram, Christy P. George, Himanshu Sharma, Kakasaheb R. Mahadik, Sharvil Patil, Kumar Vanka, S. Arulmozhi and Rajesh G. Gonnade, Rivaroxaban eutectics with improved solubility, dissolution rates, bioavailability and stability, CrystEngComm, 2023,25, 3253-3263, https://doi.org/10.1039/D3CE00261F
55. Metre, S; Mukesh, S.; Samal, S.K.; Chand, M. and Sangamwar, A.T. Enhanced Biopharmaceutical Performance of Rivaroxaban through Polymeric Amorphous Solid

Dispersion, Mol. Pharmaceutics 2018, 15, 2, 652–668 https://doi.org/10.1021/acs.molpharmaceut.7b01027

56. Metre S, Mukesh S, Samal SK, Chand M, Sangamwar AT. Enhanced Biopharmaceutical Performance of Rivaroxaban through Polymeric Amorphous Solid Dispersion. Mol Pharm. 2018 Feb 5;15(2):652-668. doi: 10.1021/acs.molpharmaceut.7b01027.
57. Xu, Y.; Wu, S. P.; Liu, X. J.; Zhang, L. J.; Lu, J. Crystal characterization and transformation of the forms I and II of anticoagulant drug rivaroxaban. Cryst. Res. Technol. 2017, 52, (3)
58. Kapourani, A.; Valkanioti, V.; Kontogiannopoulos, K. N.; Barmpalexis, P. Determination of the physical state of a drug in amorphous solid dispersions using artificial neural networks and ATR-FTIR spectroscopy, Int. J. Pharmaceutics: X, 2, 2020, 100064, https://doi.org/10.1016/j.ijpx.2020.100064.
59. Xu, Y.; Wu, S.-P.; Liu, X.-J.; Zhang, L.-J. and Lu, J. Crystal characterization and transformation of the forms I and II of anticoagulant drug rivaroxaban, Cryst. Res. Technol. 52, No. 3, 1600379 (2017) / DOI 10.1002/crat.201600379
60. Bhattacharyya, S.; Ghosh, H.; Covarrubias-Zambrano, O.; Jain, K.; Swamy, K.V.; Kasi, A.; Hamza, A.; Anant, S.; VanSaun, M.; Weir, S.J.; et al. Anticancer Activity of Novel Difluorinated Curcumin Analog and Its Inclusion Complex with 2-Hydroxypropyl-β-Cyclodextrin against Pancreatic Cancer. *Int. J. Mol. Sci.* **2023**, *24*, 6336. https://doi.org/10.3390/ijms24076336
61. Musuc, A.M., Dumitru, R., Stan, A. et al. Synthesis, characterization and thermoreactivity of some methylcellulose–zinc composites. J Therm Anal Calorim 120, 85–94 (2015). https://doi.org/10.1007/s10973-015-4415-5
62. Dong H., Ding Q., Jiang Y., Li X., Han W. Pickering emulsions stabilized by spherical cellulose nanocrystals. Carbohyd. Polym. 2021;265:118101. doi: 10.1016/j.carbpol.2021.118101
63. Meyabadi T.F., Dadashian F., Sadeghi G.M.M., Asl H.E.Z. Spherical cellulose nanoparticles preparation from waste cotton using a green method. Powder Technol. 2014;261:232–240. doi: 10.1016/j.powtec.2014.04.039

64. Lam N.T., Saewong W., Sukyai P. Effect of varying hydrolysis time on extraction of spherical bacterial cellulose nanocrystals as a reinforcing agent for poly(vinyl alcohol) composites. J. Polym. Res. 2017;24:71.
65. Azrina Z.A.Z., Beg M.D.H., Rosli M.Y., Ramlib R., Junadi N., Alam A.K.M.M. Spherical nanocrystalline cellulose (NCC) from oil palm empty fruitbunch pulp via ultrasound assisted hydrolysis. Carbohyd. Polym. 2017;162:115–120. doi: 10.1016/j.carbpol.2017.01.035
66. Purkait B.S., Ray D., Sengupta S., Kar T., Mohanty A., Misra M. Isolation of cellulose nanoparticles from sesame husk. Ind. Eng. Chem. Res. 2011;50:871–876. doi: 10.1021/ie101797d
67. Oh S.Y., Dong I.Y., Shin Y., Hwan C.K., Hak Y.K., Yong S.C., Won H.P., Ji H.Y. Crystalline structure analysis of cellulose treated with sodium hydroxide and carbon dioxide by means of X-ray diffraction and FTIR spectroscopy. Carbohyd. Res. 2005;340:2376–2391. doi: 10.1016/j.carres.2005.08.007
68. Ayouch I., Barrak I., Kassem I., Kassab Z., Draoui K., Achaby M.E. Ultrasonic-mediated production of carboxylated cellulose nanospheres. J. Environ. Chem. Eng. 2021;9:106302. doi: 10.1016/j.jece.2021.106302
69. Zhu P, Feng L, Ding Z, Bai X. Preparation of Spherical Cellulose Nanocrystals from Microcrystalline Cellulose by Mixed Acid Hydrolysis with Different Pretreatment Routes. Int J Mol Sci. 2022 Sep 15;23(18):10764. doi: 10.3390/ijms231810764
70. Metre S, Mukesh S, Samal SK, Chand M, Sangamwar AT. Enhanced Biopharmaceutical Performance of Rivaroxaban through Polymeric Amorphous Solid Dispersion. Mol Pharm. 2018 Feb 5;15(2):652-668. doi: 10.1021/acs.molpharmaceut.7b01027
71. Shaligram, P.S.; George, C.P.; Sharma, H.; Mahadik, K.R.; Patil, S.; Vanka, K.; Arulmozhi, S. and Gonnade, R.G. Rivaroxaban eutectics with improved solubility, dissolution rates, bioavailability and stability, CrystEngComm, 2023,25, 3253-3263, https://doi.org/10.1039/D3CE00261F
72. Musuc AM, Anuta V, Atkinson I, Popa VT, Sarbu I, Mircioiu C, Abdalrb GA, Mitu MA, Ozon EA. Development and Characterization of Orally Disintegrating Tablets Containing a Captopril-Cyclodextrin Complex. *Pharmaceutics*. 2020; 12(8):744. https://doi.org/10.3390/pharmaceutics12080744

73. Zhu P, Feng L, Ding Z, Bai X. Preparation of Spherical Cellulose Nanocrystals from Microcrystalline Cellulose by Mixed Acid Hydrolysis with Different Pretreatment Routes. Int J Mol Sci. 2022 Sep 15;23(18):10764. doi: 10.3390/ijms231810764
74. Ren R.W., Chen X.Q., Shen W.H. Preparation and separation of pure spherical cellulose nanocrystals from microcrystalline cellulose by complex enzymatic hydrolysis. Int. J. Biol. Macromol. 2022;202:1–10. doi: 10.1016/j.ijbiomac.2022.01.009
75. Guo J., Guo X.X., Wang S.Q., Yin Y.F. Effects of ultrasonic treatment during acid hydrolysis on the yield, particle size and structure of cellulose nanocrystals. Carbohyd. Polym. 2016;135:248–255. doi: 10.1016/j.carbpol.2015.08.068
76. Anwer, M.K.; Mohammad, M.; Iqbal, M.; Ansari, M.N.; Ezzeldin, E.; Fatima, F.; Alshahrani, S.M.; Aldawsari, M.F.; Alalaiwe, A.; Alzahrani, A .A.; Aldayel, A.M. Sustained release and enhanced oral bioavailability of rivaroxaban by PLGA nanoparticles with no food effect, Journal of Thrombosis and Thrombolysis, 49 (2020) 404-412
77. Zhao,Y.; Sun, C.; Shi, F.; Firempong, C.K.; Yu, J.; Xu X.; Zhang, W. (2016) Preparation, characterization, and pharmacokinetics study of capsaicin via hydroxypropyl-beta-cyclodextrin encapsulation, Pharmaceutical Biology, 54:1, 130-138, DOI: 10.3109/13880209.2015.1021816
78. Cheng, M.; Qin, Z.; Liu, Y.; Qin, Y.; Li, T.; Chen, L.; Zhu, M. Efficient extraction of carboxylated spherical cellulose nanocrystals with narrow distribution through hydrolysis of lyocell fibers by using ammonium persulfate as an oxidant, J. Mater. Chem. A, 2014,2, 251-258, https://doi.org/10.1039/C3TA13653A.
79. Gill P., Moghadam T.T., Ranjbar B. Differential scanning calorimetry techniques: applications in biology and nanoscience. J Biomol Tech. 2010 Dec;21(4):167-93.
80. Ainurofiq A., Choiri S. Development and optimization of a meloxicam/β-cyclodextrin complex for orally disintegrating tablet using statistical analysis. Pharm Dev Technol. 2018 Jun;23(5):464-475. doi: 10.1080/10837450.2016.1264418.
81. van der Merwe J, Steenekamp J, Steyn D, Hamman J. The Role of Functional Excipients in Solid Oral Dosage Forms to Overcome Poor Drug Dissolution and Bioavailability. Pharmaceutics. 2020 Apr 25;12(5):393. doi: 10.3390/pharmaceutics12050393.
82. Sarabia-Vallejo, Á.; Caja, M.d.M.; Olives, A.I.; Martín, M.A.; Menéndez, J.C. Cyclodextrin Inclusion Complexes for Improved Drug Bioavailability and Activity:

Synthetic and Analytical Aspects. *Pharmaceutics* **2023**, *15*, 2345. https://doi.org/10.3390/pharmaceutics15092345

83. S. Gao, C. Bie, Q. Ji, H. Ling, C. Li, Y. Fu, L. Zhao, F. Ye, Preparation and characterization of cyanazine–hydroxypropyl-beta-cyclodextrin inclusion complex, RSC Advances 9(45), (2019), 26109-26115, DOI: 10.1039/C9RA04448E
84. Rowe, R. C. York, P. Colbourn, E.A. Roskilly, S. J. The influence of pellet shape, size and distribution on capsule filling—A preliminary evaluation of three-dimensional computer simulation using a Monte-Carlo technique, International Journal of Pharmaceutics, Volume 300, Issues 1–2, 2005, Pages 32-37, https://doi.org/10.1016/j.ijpharm.2005.05.007
85. Chopra, R.; Podczeck, F.;Newton, J.M.; Alderborn, G. The influence of pellet shape and film coating on the filling of pellets into hard shell capsules, European Journal of Pharmaceutics and Biopharmaceutics, Volume 53, Issue 3, 2002, Pages 327-333, https://doi.org/10.1016/S0939-6411(02)00015-2
86. Isabelle Husson, Bernard Leclerc, Gilles Spenlehauer, Michel Veillard, Francis Puisieux, Guy Couarraze, Influence of size polydispersity on drug release from coated pellets, International Journal of Pharmaceutics, 86 (2–3), 1992, 113-121, https://doi.org/10.1016/0378-5173(92)90187-7
87. Ulusoy, U. A Review of Particle Shape Effects on Material Properties for Various Engineering Applications: From Macro to Nanoscale. Minerals 2023, 13, 91. https://doi.org/10.3390/min13010091.
88. De Leersnyder F., Peeters E., Djalabi H., Vanhoorne V., Van Snick B., Hong K., Hammond S., Liu A.Y., Ziemons E., Vervaet C., Grymonpré W., Verstraete G., Vanhoorne V., Remon J.P., De Beer T., Vervaet C., De Beer T. Development and validation of an in-line NIR spectroscopic method for continuous blend potency determination in the feed frame of a tablet press . *J. Pharm. Biomed. Anal*. 2018, 151: 274-283 DOI: 10.1016/j.jpba.2018.01.032
89. Juan G. Osorio, Fernando J. Muzzio, Evaluation of resonant acoustic mixing performance, *Powder Technology*, 78, 2015, 46-56, https://doi.org/10.1016/j.powtec.2015.02.033
90. Kurihara K, Ichikawa I. Effect of powder flowability on capsule-filling-weight-variation. *Chem Pharm Bull.* 1978;26:1250–1256

91. Kang JH; Lee JE; Jeong SJ; Park CW; Kim DW; Weon KY. Design and optimization of rivaroxaban-cyclodextrin-polymer triple complex formulation with improved solubility. *Drug Design, Development and Therapy* 2022, 16, 4279-4289, doi:10.2147/dddt.S389884
92. Kushwah V; Arora S; Tamás Katona M; Modhave D; Fröhlich E; Paudel A. On absorption modeling and food effect prediction of rivaroxaban, a BCS II drug orally administered as an immediate-release tablet. *Pharmaceutics* **2021**, *13*, 283, doi:doi:10.3390/pharmaceutics13020283
93. Fahmy R; Martinez MN. Primer on the science of in vitro dissolution testing of oral dosage forms and factors influencing its biological relevance. *Dissolution Technologies* **2019**, *26*, 14-26, doi:10.14227/DT260119P14
94. Sherje AP; Jadhav M. B-cyclodextrin-based inclusion complexes and nanocomposites of rivaroxaban for solubility enhancement. *Journal of Materials Science: Materials in Medicine* 2018, 29, 186, doi:10.1007/s10856-018-6194-6
95. Medarević D; Kachrimanis K; Djurić Z; Ibrić S. Influence of hydrophilic polymers on the complexation of carbamazepine with hydroxypropyl-β-cyclodextrin. *European Journal of Pharmaceutical Sciences* 2015, 78, 273-285, doi:10.1016/j.ejps.2015.08.001

Declaration of interests

☒ The authors declare that they have no known competing financial interests or personal relationships that could have appeared to influence the work reported in this paper.

☐ The authors declare the following financial interests/personal relationships which may be considered as potential competing interests: